

A monopole microwave-assisted electrochemical sensor for the detection of liquid chemicals

A. Karatepe^b, O. Akgöl^b, Y. I. Abdulkarim^c, Ş. Dalgac^d, H. N. Awl^e,
F. F. Muhammadsharif^f, M. Karaaslan^b, E. Ünal^b, S. Raza Saeed^g, H. Luo^a,
S. X. Huang^{a,*}

^a*School of Physics and Electronics, Central South University, Changsha, Hunan 410083, China.*

^b*Department of Electrical and Electronics, Iskenderun Technical University, Hatay, 31100, Turkey*

^c*Medical Physics Department, College of Medicals & Applied Science, Charmo University, 46023, Chamchamal, Sulaimania, Iraq*

^d*Department of Electric and Electronics engineering, Sivas University of Science and Technology, 58050 Sivas, Turkey*

^e*Department of Communication, Engineering College, Sulaimani Polytechnic University, 46001 Sulaimani, Iraq*

^f*Department of Physics, Faculty of Science and Health, Koya University, 44023 Koya, Iraq*

^g*Charmo Centre for Research, Training and Consultancy, Charmo University, 46023 Chamchamal, Iraq*

In this paper, a new sensor structure is presented based on a printed circuit board (PCB) monopole antenna with operating frequency of $f = 2$ GHz. Numerical investigation was performed in order to determine the ethanol alcohol ratio in wine and isopropyl alcohol ratio in disinfectants (sanitizers). Finite Integration Technique (FIT) based commercial high-frequency electromagnetic solver CST Microwave Studio has been used for the simulation study. The loss tangent values and dielectric constants of the samples used in the current study were obtained by KEYSIGHT brand PNA-L N5234A Network Analyzer. The proposed sensor structure was able to greatly differentiate the ethanol alcohol content in the wine and the isopropyl alcohol content in the sanitizer through the return loss values and corresponding graphs. In the design of patch antenna, the electromagnetic permittivity ratios of the samples corresponding to the alcohol ratio and isopropyl ratio are considered and the antenna dimensions along with the working frequency were optimized accordingly. In the related frequency band, permittivity values corresponding to the ethanol alcohol and isopropyl alcohol ratios exhibit a linear variation and make the sensor design possible. According to the obtained results, it was found that the changes in the resonance frequency can be associated with ethanol alcohol and isopropyl alcohol ratio inside the samples. The change of ethanol alcohol amount and isopropyl alcohol in the liquid samples tested at the resonance frequency of patch antenna is proportional to the change in the resonance frequency and they are very close to a linear characteristic.

(Received October 3, 2020; Accepted July 2, 2021)

Keywords: PCB monopole antenna, Chemical liquid, Sensing application, Dielectric characterization

1. Introduction

Nowadays, researchers are concentrating on sensor studies due to its involvement in many technological developments. For this purpose, many new techniques have been introduced in the literature to provide more sensing capability and real time response. Most of these sensors are designed in a way to be fabricated from low cost PCBs (printed circuit boards) and easily integrated

* Corresponding author: hsx351@csu.edu.cn

within the proposed sensor systems. Finite Difference Time Domain (FDTD) is employed to model and simulate of the antenna and metamaterial designs [1], in this work we have used CST (computer simulation technology) to simulate and design proposed structure. In order to achieve an effective electromagnetic response, subwavelength resonators are normally used in the designs [2]. Usually, the working principle of the sensors is based on electrical variation of the samples. When a small electrical variation is observed at the sensor layer of the designed structure, the corresponding frequency shifts to upper or lower frequencies. Therefore, these proposed structures are considered as a high sensitivity design and can be effectively used to detect small amount of sample changes at Microwave terahertz frequencies [3-5]. The authors and his colleagues in [6-8] and [9, 10] presented a compact metamaterial sensor to observe liquid properties. The proposed designs were used for various applications including micro-fluid, strain and rotation sensing. Other sets of multifunction sensors were proposed in [11-13], which can be used for different types of application such as humidity, pressure, thickness, density and temperature sensing. These designs were based on printed transmission line, which helps easy integration with other circuit parts of the system.

In the presented designs, the sensors were designed separately and integrated with the other parts of the system. However, as the technologies developed, the demand for smaller devices has been increasing. Therefore, researchers have tried to make the antennas and sensors as a single unit to eliminate substrate integration issues and provide wireless communication capabilities in sensor systems [14]. In [15], Cylindrical Dielectric Resonator Antenna-Based Sensors were proposed to be used for liquid monitoring. The design was successfully used for both sensing and antenna applications with a high quality factors and good impedance matching at the resonance frequency. Metamaterial monopole antenna was presented in [16] to be used for sensing applications. The resonance frequency at 1.35 GHz, significantly changes when different types of water are tested. In [17], a Microstrip patch antenna was designed for temperature sensing. The antenna system consists of a classical microstrip patch antenna mounted on a metallic base with the addition of two slots in the metallic base operated at 5 GHz and 6 GHz. Another temperature sensing reconfigurable antenna was presented in [18]. The antenna sensor has an effective temperature sensing range from 170 °C to 700 °C, which is suitable for wireless sensing network applications. An electromagnetic bandgap (EBG) structure based on patch resonator was proposed in [19, 20]. The metamaterial patches bonded with a polydimethylsiloxane (PDMS) cavity was used for adulteration detection in oil. Another liquid antenna sensor was designed based on EBG structure. In the design, a CPW (coplanar waveguide) feed monopole antenna was mounted on EBG structure. When the dielectric properties of the liquid samples vary, the reflected phase of the EBG changes. This variation in the phase of the surface wave leads to a change in the reflection coefficient [21]. Monopole antennas, which can also be built as microstrip line, are presented as sensors in different application fields such as health, geophysical and technological devices. In [22], a new model based on the differences in electrical properties between healthy and malignant tissues in microwave detection of breast cancer was presented. In [23], a monopolar antenna (monopolar) operating in the range of 100 MHz to 2 GHz was designed for the field measurements of liquid water content in both soil and snow as an alternative to capacitive sensors used in soil and snow wetness measurements. In this study, it is emphasized that unipolar probe is a very suitable and practical dielectric sensor for wetness measurements of different porous grain geophysical materials such as soil or snow. In [24], a new monopole antenna study was presented for high-voltage equipment insulation, intense electric fields, chemical reactions, mechanical stresses, temperature changes and various environmental events due to exposure to stressful conditions reported that partial discharges, which are defined as electrical discharges, may occur, and therefore a new monopole antenna model was applied to monitor partial discharging activity in high-voltage insulation systems.

In this work, a new design monopole antenna sensor is presented by using CST microwave studio which is a Finite Integration Technique (FIT) based high-frequency electromagnetic solver. According to the numerical results, the proposed sensor structure is successfully designed for the real-time, fast and accurate detection of ethanol and isopropyl alcohol as a biochemical sensor for wine-ethanol and disinfectant-isopropyl mixtures. The rest of this paper is organized as follows: in section 2, the methodology of the suggested design structure is presented, followed by the achieved chemical liquid sensor study and measurement of electrical properties, results and elaborated

discussion in the following sections. Finally, the main conclusions of this work are drawn and given in Section 6.

2. Design structure of PCB Monopole Antenna

A novel monopole antenna sensor structure based on printed circuit board (PCB) at 1-3 GHz microwave frequency range was designed for the purpose of sensing applications as shown in Figure 1. Finite Integration Technique (FIT) based CST microwave studio was used for the simulation study. In simulations, FR4 (Flame Retardant 4) has been assigned as the substrate material type for the PCB monopole antenna structure with the thickness of 1.6 mm, loss tangent value of 0.02, dielectric permeability of 4.2 and magnetic permeability of 1. The surface of the structure which is made of copper type metal with a thickness of 0.035 mm and has an electrical conductivity of $5.8001 \times 10^7 \text{ S/m}$. The designed structure is compatible with X-band. Detailed view of the dimensions of the designed antenna is shown in Fig. 1. The geometric dimensions of the PCB based monopole antenna liquid sensor are determined by genetic algorithm and parametric study. In simulation results for the proposed monopole antenna structure, S_{11} parameter (return loss) has been obtained and shown in Figure 6. One can see from the figure that the resonance frequency is around $f = 2 \text{ GHz}$ and the antenna has a very good far field radiation pattern at this operation frequency. The advantage of this designed structure is that it is small in size and cost effective and it can be used in many practical application areas.

As shown in Fig. 1, the length of our antenna is 36 mm and the thickness of the microstrip line is 3 mm. The radius of the copper ground plane was chosen as $r = 18 \text{ mm}$.

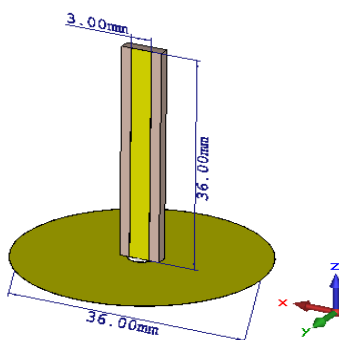


Fig. 1. Detailed view of PCB monopole antenna.

For the numerical analysis and for measuring the proposed structure, the monopole antenna with sample holder structure was designed after the parametric study which was carried out by the electromagnetic simulation software. In Fig. 6, the return loss (S_{11} parameters) for this structure has the value of -8.4 dB at $f = 2 \text{ GHz}$. The minimum scattering parameter in this frequency range indicates that energy transmission is at the highest level, the final version of the part to be dipped into the sample contents with appropriate sizes was prepared. The illustrations of the antenna with the sample are shown in Fig. 2 (a). The measurement is performed by immersing the tip of the antenna into the sample. As shown in Fig. 2 (b), the upper part of the antenna is covered with a plastic layer so that it does not come into contact with the liquid. For better understanding of antenna orientation, both plastic coated and uncoated versions of the measurement are shown in Fig. 2 (a), (b). It was considered that the antenna was immersed 20 mm into the samples consisting of wine-ethanol and disinfectant-isopropyl mixture and the results were obtained accordingly.

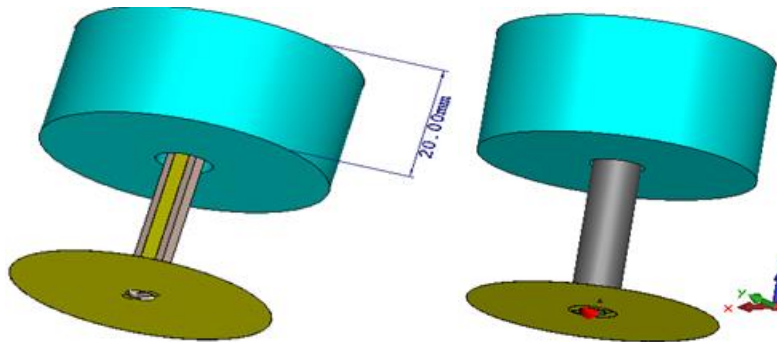


Fig. 2. PCB monopole antenna uncoated (a) and coated (b) with plastic.

3. Chemical Liquid Sensor Study and Measurement of Electromagnetic Properties of the samples

In this section, the electrical performance of PCB monopole antenna-based sensor is analyzed and discussed for the case of detecting the ethanol alcohol content in wine and isopropyl alcohol in disinfectant samples. The proposed structure was realized with a designed Printed Circuit Board (PCB) based monopole antenna. In the first step of our investigations, the electrical properties of ethanol alcohol content in wine and isopropyl alcohol in disinfectant were measured by KEYSIGHT brand PNA-L N5234A Network Analyzer and a compatible dielectric probe equipment. The loss tangent values and dielectric constants of the samples that we prepared show proportional changes in the X band frequency range. Based on the measurement results, it was seen that there are different resonance frequency values in each proportional change. The vector network analyzer (VNA) also detects the real and imaginary parts of the relative permeability values known as the dielectric constant and the loss tangent for the proportions in the samples tested. The dielectric constant can be expressed as energy stored in the material relative to an external electric field. The imaginary part of the dielectric constant occurs in the outer part of the material of the electric fields due to energy losses. The loss tangent value which is an important parameter of the system is determined by the ratio of the real and the imaginary part of the dielectric constant.

3.1. Investigating the Electromagnetic Properties of the Samples

The dielectric measurement setup of the selected samples at different rates using the vector network analyzer are shown in Fig. 3. Before conducting the measurements, the analyzer needs to be calibrated. Frequency range of 1-5 GHz is defined on the VNA. In the first step of the calibration pure water at room temperature at around 22°C is used for the dielectric probe. The air is tested while the dielectric probe is left in open air. As the final step, a shorting apparatus is used to short the probe tips and the calibration is completed. Since we know the dielectric constant of water as well as air, they are measured again and the results are controlled in order to ensure correct calibration of the device. When we measure the value of the water which is known to have dielectric constant of about 80, it was checked if the curve is around that specific value in the operation frequency band. After the preliminary preparations are completed, the next stage is proceeded and homogeneous samples are prepared in different proportions and sample measurements are initiated. According to the measurements, results of the ethanol alcohol amount in wine and the amount of isopropyl alcohol in disinfectant are obtained and shown in the tables and dielectric graphs.

3.1.1 Electromagnetic Properties of Wine-Ethanol Mixture

The dielectric probe was employed to measure the dielectric parameters of the samples at the operating frequency of 1-5 GHz. Table 1 shows the dielectric constants and loss tangent values obtained for different contents of wine-ethanol ratio. The dielectric measurement was carried out at room temperature and the real part (ϵ'), the imaginary part (ϵ''), and the loss tangent ($\tan \delta = \epsilon''/\epsilon'$) values were found by the ratio depending on ethanol content for the proposed antenna sensor structure. From the simulation results obtained for S_{11} parameter, the resonance frequency is about 2

GHz and the operation frequency range was selected as 1-5 GHz in terms of the previously determined dielectric constant values shown in Table 2.

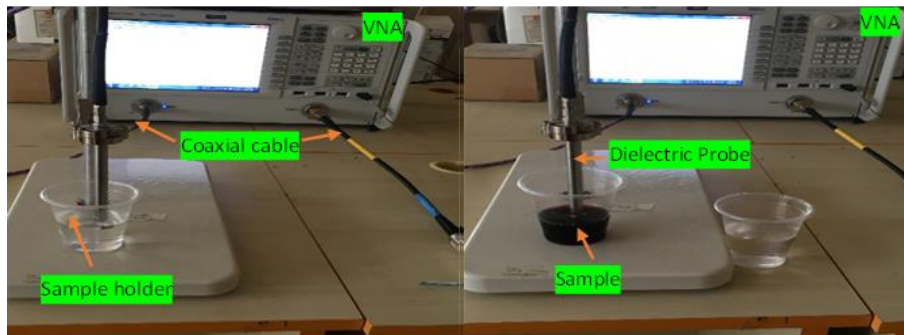


Fig. 3. Experimental measurement setup for determination of electrical characteristics of the samples.

Table 1. Values of the electrical characteristics ethanol alcohol ratio in wine.

Wine + Ethanol Content (%)	ϵ'	ϵ''	Tan δ
15	63,18	23,84	0.377
25	52,33	24,96	0.476
35	43,97	24,63	0.560

Table 1 shows that different dielectric constant and loss tangent values are obtained at the same frequency range by varying the density of ethanol percentage in wine sample among 15, 25 and 35 percentage, respectively. For example, the dielectric constants of the samples with optimum 15% ethanol and 25% ethanol show real values at the frequency of 2 GHz which are around 63.18 and 52.33, respectively. It is seen that as the amount of ethanol in the sample content increases, a linear decrease occurs in the real part (ϵ') of the electrical permittivity and loss tangent (tan δ) value, which is the expression of the electromagnetic wave energy lost during the transmission.

In addition, the frequency band from 1 GHz to 5 GHz are selected according to the value in the Table 2. When the frequency applied increases, it is seen that the dielectric constant values decrease. The dielectric graph of the samples containing ethanol at the specified ratios in wine samples for the frequency range of 1-5 GHz is illustrated in Fig. 4.

Table 2. Dielectric constant values for wine-ethanol.

Frequency (GHz)	Dielectric Constant (ϵ)		
	%15	%25	%35
1	71.98	64.04	57.72
2	70.12	61.53	54.62
3	67.82	58.40	50.85
4	65.18	54.89	46.80
5	62.12	51.01	42.54

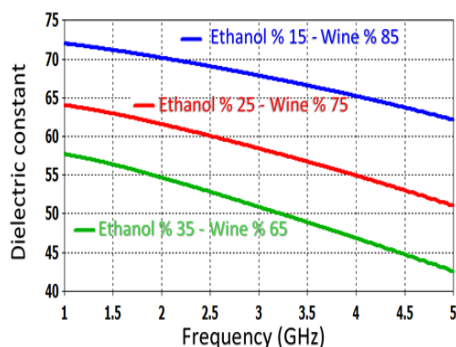


Fig. 4. Dielectric values for different contents of wine-ethanol in the frequency range from 1 to 5 GHz.

3.2.2. Electromagnetic Properties for Disinfectant-Isopropyl

In this part of this study, the amount of isopropyl alcohol in the disinfectant-isopropyl samples were measured by the dielectric probe connected to the network analyzer as shown in Table 3. The dielectric constant values are obtained from the measurement at room temperature. In the tables, the real value (ϵ'), the imaginary value (ϵ'') and the loss tangent ($\tan \delta = \epsilon''/\epsilon'$) can be seen. The Monopole microstrip antenna was designed for $f=2$ GHz and the electromagnetic characteristics of the sample for the same frequency was used and shown in Table 3 for the frequency of 2 GHz where the antenna based sensor provides the most energy transmission.

According to the results of the laboratory simulation study depending on the isopropyl content at the frequency of 2 GHz, dielectric and loss tangent ($\tan \delta$) values are presented in Table 3.

Table 3. Values of the electrical characteristics Isopropyl alcohol ratio in disinfectant.

Disinfectant + Isopropyl Content (%)	ϵ'	ϵ''	Tan δ
70	13.33	11.57	0.867
80	9.59	8.35	0.870
90	7.37	6.09	0.826

When Table 3 is examined, the proportional increase in the disinfectant isopropyl-containing samples in the same frequency range leads to a linear-like decrease in dielectric constant and loss of tangent values. For example, the real values (ϵ') of the dielectric constants of the samples containing 70% isopropyl and 80% isopropyl at the operating frequency of 2 GHz have the values of 13.33 and 9.59, respectively. As the amount of isopropyl increases in the sample content, a linear decrease is observed in the real value (ϵ') and the loss tangent ($\tan \delta$) values which are the expression of the electromagnetic wave energy lost during the transmission. In addition, 1-5 GHz operating frequency range was selected according to the values given in Table 4. When the applied frequency increases, a decrease is seen in the dielectric constant values.

Table 4. Dielectric constant values for disinfectant-isopropyl at 1-5 GHz.

Frequency (GHz)	Real Dielectric Coefficients (ϵ)		
	%70	%80	%90
1	27.38	21.16	16.37
2	21.48	15.48	11.42
3	17.45	12.37	9.20
4	14.73	10.50	7.95
5	12.68	9.16	7.09

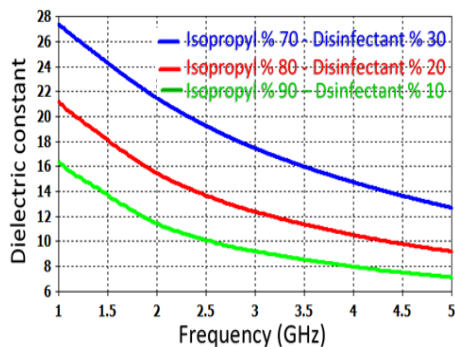


Fig. 5. Dielectric values for disinfectant-isopropyl in the range of 1-5 GHz.

5. Simulated Results and Discussion

5.1. Simulated results for PCB Monopole Antenna Wine-Ethanol sample

CST electromagnetic simulation program was used for the analysis of the designed sensor structure. A discrete port is defined in the simulation program instead of waveguide port to make it more realizable for a monopole antenna. The graph of S_{11} parameter, which we define it as the return loss obtained by optimizing our antenna, is shown in Fig. 6.

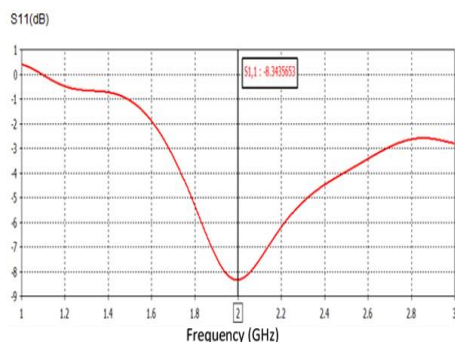


Fig. 6. Return loss graph of PCB monopole antenna (S_{11}).

As can be seen, the designed monopole antenna resonates at a frequency of $f = 2$ GHz. The highest energy transmission took place at this particular frequency point. In addition, the far field gain from the polar graph given in Fig. 7 is $G = 1.81$ dBi and the half power beam width is determined as $HPBW = 88.2^\circ$.

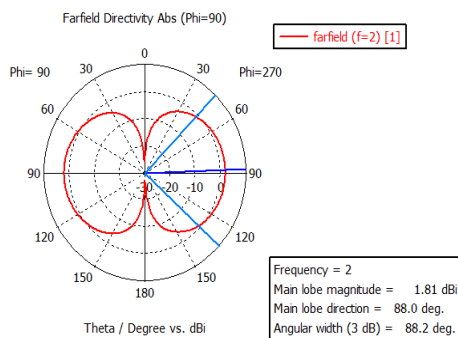


Fig. 7. Propagation pattern of PCB monopole antenna.

New materials were defined in the simulation in order to perform the studies by immersing the tip of the monopole antenna which was designed by using the obtained dielectric constant values and the lost tangent values. Simulations were carried out by using these new materials. Simulation studies were carried out by placing the designed antenna into samples with different proportions of ethanol by 20 mm. The part of the antenna to be dipped into the sample is coated with plastic to prevent contact of the antenna with the liquid. In order to determine if the tangent values and dielectric constants of the samples show proportional changes or not, KEYSIGHT brand PNA-L Network Analyzer which is capable of measuring as high as 43 GHz and dielectric probe apparatus were used. S_{11} graphs and resonance frequency shifts in sensor design due to various percentages of mixtures containing ethanol in wine and isopropyl alcohol in disinfectant are given.

Simulation studies were started with a sample containing 15% ethanol and ethanol was added into the samples by 10% increments. Measurements of the samples formed by increasing the amount of ethanol in wine by 10% are shown in Table 6. Resonance frequency shifts in sensor design due to ethanol percentages in wine-ethanol samples are given in Fig. 8.

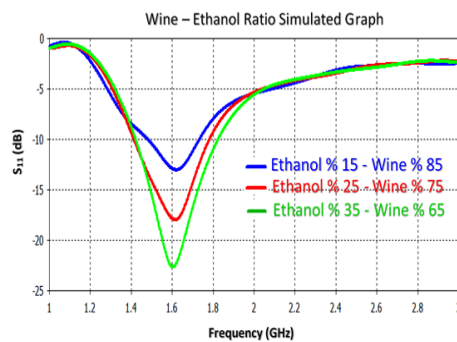


Fig. 8. PCB monopole antenna wine-ethanol simulation chart.

Table 5 shows that the changes in the resonance frequency of the samples in terms of various percentage of the ethanol-alcohol ratio are linear. As a result of this linearity, a total bandwidth of 16 MHz is achieved. 16 MHz band allows us to easily and precisely estimate intermediate values of the contents of our liquid samples. The resonance value for the sample containing 15% ethanol is $f = 1.620$ GHz. As the content of ethanol increases to 35% ethanol, which is our most concentrated sample, shifts to $f = 1.604$ GHz. In addition, the amplitude values also show a significant change which is also close to linear.

Table 5. Resonance frequency, return loss (S_{11}) and dielectric constants depending on the amount of ethanol monopole antenna.

Wine + Ethanol Content (%)	Resonance Frequency (GHz)	S11 value (dB)	ϵ'	ϵ''	$\tan\delta$
15	1,620	-13,025	70,12	13,36	0,190
25	1,614	-17,985	61,53	14,14	0,229
35	1,604	-22,661	54,62	14,62	0,267

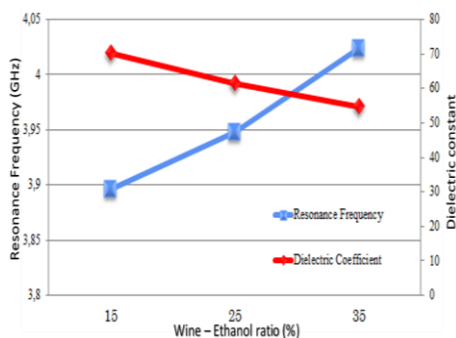


Fig. 9. Variation of the resonance frequency of the PCB Monopole antenna sensor depending on the ethanol ratio in wine.

The changes in the resonance frequency caused by the increase in the ethanol-alcohol ratio in the samples are proportional to the dielectric constant values and a linear change can be seen in the concentration distribution graph in Fig. 9. The interval between the increments of 10% ethanol and the changing structure show us that the intermediate values can be estimated. The electrical size, which varies according to the varying frequency, is small enough to detect these mixtures. This shows that the antenna-based sensor that we have designed is a bio-sensor suitable for detecting the ethanol content in wine.

5.2. Simulation results for PCB Monopole Antenna Disinfectant-Isopropyl sample

Simulation studies were started with 70% isopropyl sample and additions with 10% increments were made in order to show the changes in the return loss curves. According to the simulation results of samples obtained by increasing the amount of isopropyl in disinfectant by 10%, the values of the resonance frequency shifts in the sensor design depending on the percentages of the mixtures are given in Table 6. Figure 10 shows the resonance frequency shifts in sensor design due to isopropyl percentages in disinfectant-isopropyl samples.

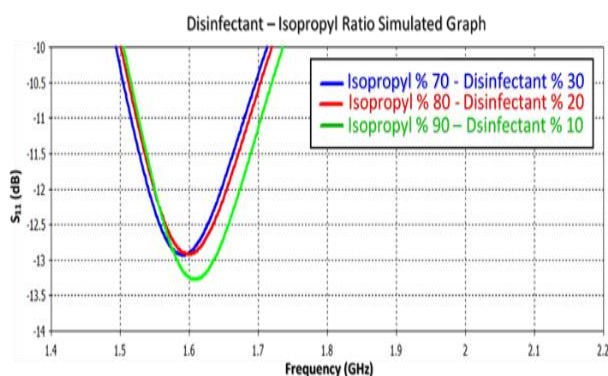


Fig. 10. PCB monopole antenna disinfectant-isopropyl simulation chart.

Table 6 shows the changes in the resonance frequency of the samples according to the isopropyl alcohol ratio and it is noteworthy that this change shows a significant linearity. It can be seen from these results that the sensor has a total of 18MHz detection bandwidth. 18 MHz band allows us to easily and precisely estimate intermediate values on the detection bandwidth. The resonance frequency value for the sample containing 70% isopropyl refers to $f = 1.590$ GHz. As the isopropyl content increases, it is observed that the resonance value shifts to higher values, for example $f = 1.608$ GHz for 90% isopropyl content which is the most concentrated sample.

Table 6. Amount of isopropyl and dielectric constant of the samples, resonance frequency and S_{11} of the monopole antenna.

Disinfectant + Isopropyl Content (%)	Resonance Frequency (GHz)	S11 value (dB)	ϵ'	ϵ''	$\tan\delta$
70	1,590	-12,929	21,48	11,70	0,544
80	1,598	-12,919	15,48	9,94	0,642
90	1,608	-13,274	11,43	8,17	0,714

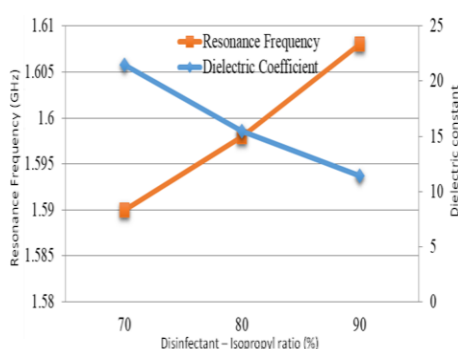


Fig. 11. Variation of the resonance frequency with isopropyl ratio in disinfectant for the PCB Monopole antenna sensor.

The resonance frequency changes caused by the increase in the isopropyl alcohol ratio in the samples are proportional to the dielectric constant values and the change is linear. The interval between the samples having the highest and lowest isopropyl ratios with an increase rate of 10% shows us that the intermediate values can be estimated thank to the linear changes determined in the resonance frequency points due to linearly varying content ratios. The electrical size, which varies according to the frequency, is small enough to detect these mixtures. This shows that the antenna-based sensor that we have designed is a bio-sensor suitable for detecting the ethanol content in wine.

6. Conclusions

In conclusion, a new design monopole antenna based PCB (Printed Circuit Board) are presented numerically in the frequency range 1-5 GHz for sensing application. Finite Integration Technique (FIT) based CST microwave studio was used for simulation study. According to numerical analysis, it was observed that the resonance frequency changed linearly according to the samples formed by increasing the 10% ethanol alcohol in wine and isopropyl alcohol in disinfectant.

As a result of this linearity, it is seen that there is a detection band width of 16 MHz and 18 MHz respectively. We can say that this change can be used for precise detection. In addition to these changes, it was determined that the amplitude values of the return loss S_{11} parameter could be used to determine the amount of ethanol in the wine samples with a near linear change of approximately 9 dB and 0.5 dB. respectively We can say that this change can be used for precise detection. The proposed structure was designed successfully accomplished the ethanol detection process in real time, quickly and accurately as a biochemical sensor.

Author Contributions: “conceptualization, A.K., Y.I.A. and S.D.; methodology, A.K. and S.D.; software, A.K. and S.D.; validation, M.K., L.D. and Y.I.A.; formal analysis, Y.I.A, H.N.A and F.F.M.; investigation, A.K., Y.I.A. and S.D.; resources, F.F.M. and E.U.; data curation, H.N.A. and E.U.; writing—original draft preparation, Y.I.A. and A.K.; writing—review and editing, H.N.A,F.F.M, E.U. and S.R.S ; visualization A.K. and S.D. ; supervision, O.A. M.K. and Y.I.A.; project administration, O.A. , M.K. and H.L. ; funding acquisition SH.H.”,

Funding

This work was supported by the National Key Research and Development Program of China (Grant no.2017YFA0204600), the National Natural Science Foundation of China (Grant no. 51802352) and the Fundamental Research Funds for the Central Universities of Central South University (Grant no.2018zzts355).

Acknowledgments

The author would like to thanks for Central South University and, Iskenderun Technical University for the technical supports.

References

- [1] A. Hendi, F. Alkallas, H. Almoussa, H. Alshahri, M. Almoneef, M. Alenazy, N. Alsaif, A. Altowyan, A. Laref, M. Awad, K. Ortachi, *Digest Journal of Nanomaterials and Biostructures* **15**, 707 (2020).
- [2] H. Jung, J. Koo, E. Heo, B. Cho, C. In, W. Lee, H. Jo, J. Ho, C. Hyunyong, C. Moon, S. Kang, H. Lee, *Advanced materials* **30**(31), 1870231 (2018).
- [3] W. Withayachumnankul, K. Jaruwongrungrsee, A. Tuantranont, C. Fumeaux, D. Abbott, *Sensors and Actuators A: Physical* **189**, 233 (2013).
- [4] Y.I. Abdulkarim, L. Deng, P. Zhang, H. Luo, S. Huang, M. Karaaslan, O. Altıntaş, M. Bakır, F.F. Muhammadsharif, H. N.Awl, C. Sabah, K.S.L. Al-badri, *Journal of Materials Research and Technology* **9**(5), 10291 (2020).
- [5] Y.I. Abdulkarim, L. Deng, M. Karaaslan, O. Altıntaş, H.N. Awl, F.F. Muhammadsharif, C. Liao, E. Unal, H. Luo, *Sensors* **20**(3), 943 (2020).
- [6] A. Ebrahimi, W. Withayachumnankul, S. Al-Sarawi, D. Abbott, *IEEE Sensors* **14**(5), 1345 (2014).
- [7] A. Karatepe, O. Akgöl, Y.I. Abdulkarim, Ş. Dalgac, F.F. Muhammadsharif, H. N.Awl, L. Deng, E. Ünal, M. Karaaslan, L. Heng, S. Huang, *PLOS ONE* **15**(5), 0232460 (2020).
- [8] Y.I. Abdulkarim, L. Deng, O. Altıntaş, M. Karaaslan, E. Unal, *Physica E: Low-dimensional Systems and Nanostructures* **114**, 113593 (2019).
- [9] O. Altıntaş, M. Aksoy, O. Akgöl, E. Unal, M. Karaaslan, C. Sabah, *Electrochemical Society* **164**(12), 567 (2017).
- [10] Y. I.Abdulkarim, D. Lianwen, K. Muharrem, U. Emin, *Chemical Physics Letters* **732**, 136655 (2019).
- [11] M. Karaaslan, M. Bakır, *Progress In Electromagnetics Research* **149**, 55 (2014).

- [12] I.d.A. Rodrigues, S.M.C. Gomes, I.P.G. Fernandes, A.M. Oliveira-Brett, *Electroanalysis* **31**(5), 936 (2019).
- [13] M. Bakir, M. Karaaslan, O. Akgol, O. Altintas, E. Unal, C. Sabah, *Optik* **168**, 741 (2018).
- [14] C. Reig, E. Ávila-Navarro, *IEEE Sensors* **14**(8), 2406 (2014).
- [15] A. Iqbal, A. Smida, O.A. Saraereh, Q.H. Alsafasfeh, N.K. Mallat, B.M. Lee, *Sensors* **19**(5), 1200 (2019).
- [16] T. A.Elwi, *International Journal of RF Microwave Computer Aided Engineering* **28**(7), e21470 (2018).
- [17] J.W. Sanders, J. Yao, H. Huang, *IEEE Sensors* **15**(9), 5312 (2015).
- [18] F. Yang, Q. Qiao, J. Virtanen, A.Z. Elsherbeni, L. Ukkonen, L. Sydänheimo, *IEEE Antennas Wireless Propagation Lettter* **11**, 632 (2012).
- [19] R. Yadav, P.N. Patel, *IEEE Sensors* **16**(11), 4354 (2016).
- [20] L. Blandón-Naranjo, F.D. Pelle, M.V. Vázquez, J. Gallego, A. Santamaría, M. Alzate-Tobón, D. Compagnone, *Electroanalysis* **30**(3), 509 (2018).
- [21] S.Y. Jun, B.S. Izquierdo, E.A. Parker, *IEEE Transactions on Antennas and Propagation* **67**(5), 3366 (2019).
- [22] S.J. M., Fear E. C. , *IEEE Transactions on Microwave theory and Techniques* **53**(11), 3312 (2005).
- [23] D. A., *IEEE transactions on geoscience and remote sensing* **35**(5), 1371 (1997).
- [24] J.d.N. Cruz, A.J.R. Serres, A.C.d. Oliveira, G.V.R. Xavier, C.C.R.d. Albuquerque, E.G.d. Costa, R.C.S. Freire, *Sensors* **19**(3), 628 (2019).